Trauth, N., **Musolff, A.**, **Knöller, K.**, **Kaden, U.S.**, **Keller, T.**, **Werban, U.**, **Fleckenstein, J.H.** (2018):
River water infiltration enhances denitrification efficiency in riparian groundwater
Water Res. **130** , 185 - 199

http://dx.doi.org/10.1016/j.watres.2017.11.058

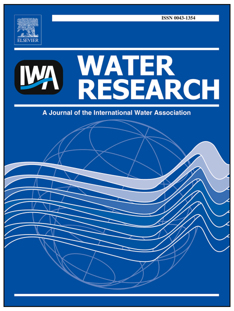

River water infiltration enhances denitrification efficiency in riparian groundwater

Nico Trauth, Andreas Musolff, Kay Knöller, Ute S. Kaden, Toralf Keller, Ulrike Werban, Jan H. Fleckenstein

PII: S0043-1354(17)30986-7

DOI: 10.1016/j.watres.2017.11.058

Reference: WR 13388

To appear in: *Water Research*

Received Date: 7 June 2017

Revised Date: 23 November 2017

Accepted Date: 27 November 2017

Please cite this article as: Trauth, N., Musolff, A., Knöller, K., Kaden, U.S., Keller, T., Werban, U., Fleckenstein, J.H., River water infiltration enhances denitrification efficiency in riparian groundwater, *Water Research* (2017), doi: 10.1016/j.watres.2017.11.058.

River water infiltration enhances denitrification efficiency in riparian groundwater

Nico Trauth[1], Andreas Musolff[1], Kay Knöller[2], Ute S. Kaden[3], Toralf Keller[1], Ulrike Werban[4], Jan H. Fleckenstein[1]

[1]Helmholtz Center for Environmental Research – UFZ, Department of Hydrogeology, Permoserstraße 15, 04318 Leipzig, Germany

[2]Helmholtz Center for Environmental Research – UFZ, Department of Catchment Hydrology, Theodor-Lieser-Straße 4, 06120 Halle (Salle), Germany

[3]Helmholtz Center for Environmental Research – UFZ, Department of Conservation Biology, Permoserstraße 15, 04318 Leipzig, Germany

[4]Helmholtz Center for Environmental Research – UFZ, Department of Monitoring and Exploration Technologies, Permoserstraße 15, 04318 Leipzig, Germany

Corresponding author: Nico Trauth, Helmholtz Center for Environmental Research – UFZ, Department of Hydrogeology, Permoserstraße 15, Leipzig, Germany, nico.trauth@ufz.de

Abstract

Nitrate contamination in ground- and surface water is a persistent problem in countries with intense agriculture. The transition zone between rivers and their riparian aquifers, where river water and groundwater interact, may play an important role in mediating nitrate exports, as it can facilitate intensive denitrification, which permanently removes nitrate from the aquatic system. However, the in-situ factors controlling riparian denitrification are not fully understood, as they are often strongly linked and their effects superimpose each other. In this study, we present the evaluation of hydrochemical and isotopic data from a 2-year sampling period of river water and groundwater in the riparian zone along a 3rd order river in Central Germany. Based on bi- and multivariate statistics (Spearman's rank correlation and partial least squares regression) we can show, that highest rates for oxygen consumption and denitrification in the riparian aquifer occur where the fraction of infiltrated river water and at the same time groundwater temperature, are high. River discharge and depth to groundwater are additional explanatory variables for those reaction rates, but of minor importance. Our data and analyses suggest that at locations in the riparian aquifer, which show significant river water infiltration, heterotrophic microbial reactions in the riparian zone may be fueled by bioavailable organic carbon derived from the river water. We conclude that interactions between rivers and riparian groundwater are likely to be a key control of nitrate removal and should be considered as a measure to mitigate high nitrate exports from agricultural catchments.

Keywords

riparian zone, nitrate contamination, nitrate stable isotopes, river-groundwater interaction, denitrification

1. Introduction

Nitrate (NO_3^-) contamination in European groundwater bodies is an increasing threat to drinking water production and ecosystem health in receiving surface waters (Grizzetti et al., 2007) with implications for agricultural and water management as well as river restoration (Gift et al., 2010). Riparian zones, that link the terrestrial and the aquatic environment, have been shown to have a significant potential for the natural attenuation of NO_3^- pollution and to function as a NO_3^- buffer zone along rivers (Hill, 1996; Puckett, 2004; Ranalli and Macalady, 2010). More specifically, in the riparian zone various nitrogen (N) species can be efficiently assimilated, transformed or permanently removed by denitrification (Clément et al., 2003; Harvey and Bencala, 1993; Hill et al., 1998; Rivett et al., 2008; Vidon and Hill, 2004a). However, denitrification rates in groundwater are not constant in space and time and are controlled by a multitude of factors (Rivett et al., 2008). Of key importance is the availability of reactants, namely NO_3^- and labile carbon for heterotrophic denitrification (Gift et al., 2010; Kaplan and Newbold, 2000; Rivett et al., 2008; Zarnetske et al., 2011) and reduced sulfur and iron(II) in the aquifer sediments for chemolithotrophic denitrification (Knöller et al., 2005; Schwientek et al., 2008). Availability of reactants in the riparian zone is facilitated by mixing of waters from different sources and of different chemical composition, namely river water with high carbon concentrations and groundwater with high NO_3^- concentrations (Baker and Vervier, 2004; Hill et al., 2000; Vervier et al., 1993). As solute transport across the river-aquifer interface is mainly advective, and controlled by the direction and the magnitude of the water fluxes across the river-groundwater interface (Vidon and Hill, 2004b), which in turn is influenced by river channel morphology and aquifer properties (Duval and Hill, 2006; Heeren et al., 2014; Wondzell and Swanson, 1999). This exchange flux of water and solutes typically varies seasonally a well as on shorter temporal scales (e.g. flood events) (Heeren et al., 2014; Sawyer et al., 2009; Trauth and Fleckenstein, 2017; Vidon et al., 2017). Since low dissolved oxygen (DO) concentrations are a prerequisite for high denitrification rates (Hedin et al., 1998; Rivett et al., 2008; Stumm and Morgan, 2012), DO depletion by aerobic reactions can control efficiency of the denitrification process (Brunke and Gonser, 1997; Diem et al., 2013a). Finally, temperature is a crucial control on the activity of both, aerobic and anaerobic bacteria. Both, the seasonal variability of temperature as well as heat exchange across the river-groundwater interface may either stimulate or suppress reaction rates (Diem et al., 2013b; Rivett et al., 2008; Vieweg et al., 2016).

In riparian zones, water flux, nutrient supply and temperature variability are often interlinked in space and time (Balestrini et al., 2016; Ranalli and Macalady, 2010). For instance high river discharges and high groundwater level often occur during the cold season, which in turn coincides with specific solute mobilization and changed river solute concentrations (Musolff et al., 2015). Consequently, disentangling these factors and their impact on N turn-over in riparian zones is challenging. During the last decades, this problem has been addressed using descriptive methods at different riparian zone types (Balestrini et al., 2016; Jacobs et al., 1988; Ranalli and Macalady, 2010). The methods used in studies to date include endmember mixing models using both, reactive and conservative solutes (Balestrini et al., 2016; Mengis et al., 1999; Pinay et al., 1998) and the use of stable isotopes of the NO_3^- molecule (Böhlke and Denver, 1995; Böttcher et al., 1990; Denk et al., 2017; Hoffmann et al., 2006; Hosono et al., 2013; Mariotti et al., 1988). Denitrification causes an enrichment of the heavier N and oxygen isotopes in the remaining NO_3^- pool. In riparian zones this technique has been applied with focus on the effect of different hydrogeological settings and land use patterns (Clément et al., 2003; Devito et al., 2000; Peter et al., 2012; Vidon and Hill, 2004b), on the implications of seasonal changes in temperature and hydrology (Cey et al., 1999; Fukada et al., 2003; Grischek et al., 1998; Pfenning and McMahon, 1997) and availability of electron donors (carbon source) and acceptors (NO_3^-) (Hedin et al., 1998; Ostrom et al., 2002).

The studies summarized above mainly used descriptive and bivariate statistics to conclude on the main factors controlling N-transformation in the riparian zone in a more *qualitative* way. Studies with a more mechanistically and *quantitative* approach focusing on factors controlling denitrification (Bu et al., 2017; Kellogg et al., 2005) and typically do not consider hydrochemical and hydrological variables at the same time providing only a limited perspective on the problem.

In this study, we present a unique two-year observational data set of spatially and temporally resolved hydrologic, isotopic and river- and groundwater quality variables, which allows a more comprehensive assessment of the interlinked processes and controls governing riparian denitrification. Samples were analyzed for stable isotopes of the NO_3^- molecule as well as for major ions, DO and dissolved organic carbon (DOC) concentration. Simultaneously, river discharge, and river and groundwater levels were measured. We applied bi- and multivariate statistics (Spearman's rank correlation and partial least squares regression) to the data to evaluate and rank the key factors that control denitrification activity in riparian groundwater at different distances from the river. By doing so, we were able to disentangle the mixed effects of seasonal temperature variations, potential hydraulic controls such as river-groundwater mixing, river discharge, and groundwater levels. This way we can provide a detailed and more comprehensive view with the focus on the spatio-temporal variations of aerobic respiration and denitrification and their mechanistic controls in the riparian zone.

2. Materials and Methods

2.1. Field site

Our field site is located at the Selke river in central Germany (51°43’37.79”N, 11°18’51.0”E) which is an intensive test site within the TERENO Harz/Central German Lowland Observatory operated by the Helmholtz Centre for Environmental Research-UFZ (Wollschläger et al., 2017) (Figure 1a) . The Selke river is part of the Bode catchment which was part of studies on catchment-scale solute export (Musolff et al., 2015) and N dynamics (Mueller et al., 2016, 2015). At the site, a 2 km long river reach of the lower Selke River, the mean annual discharge is 1.5 m^3/s. During summer base flows can be below 0.1 m^3/s. Highest discharge is typically observed during the spring snow melt season, when bankfull discharge at about 15 m^3/s and associated sediment movement can occur.

The Selke catchment covers a total area of 456 km^2. Forests dominate the upper parts of the catchment (35% of the total area) while the lowland parts are dominated by agriculture used (53% of the area). At the field site, which marks the transition from the mountainous upper catchment to the flatter, groundwater controlled lower catchment, the 2 km long river reach is lined by a strip of riparian vegetation up to 50 m wide, consisting of willow and beech trees interspersed with pasture. This strip of riparian vegetation is directly bounded by agricultural fields to the North and South of the river.

Geologically, the field site is located in the northern Harz foreland, where sandstones and limestone of the late Palaeozoic era Permian (regional names: Rotliegend and Zechstein) and the early Mesozoic era Triassic (regional names: Buntsandstein and Muschelkalk) were deposited (Bachmann et al., 2008). During the Early and Late Cretaceous the Harz was uplifted and these older sedimentary layers were eroded and steeply tilted, dipping towards the north, forming the Northern Harz Boundary Fault. At the field site the Selke river has incised into these geological units during the Plio- and Pleistocene and coincidentally deposited alluvial sediments consisting of mainly greywacke and slate stone originating from the central-east Harz mountains (Bachmann et al., 2008).

Core samples from the riparian zone obtained from a Sonic Drill Direct Push device enabled a characterization of the shallow sedimentary sequence in the riparian zone. Here, an alluvial loam, up to 1.2 m thick, covers an alluvial aquifer up to 8 m thick. The aquifer is built up of alluvial fillings that show a very heterogeneous grain size distribution ranging from silt to cobble fraction, with the main fraction of coarse sand to fine gravel. The base of the aquifer forms a clay-silt layer that acts as an aquitard. Geophysical surveys at the site (Electrical Conductivity Logging, Direct Push Injection Logging, Electrical Resistivity Tomography (Kirsch, 2008)) revealed that the thickness of the alluvial aquifer steadily decreases with distance from the Selke river.

Hydraulic conductivity (K) of the aquifer material was determined by three repeated salt tracer tests in the riparian zone, and sieve analysis of freeze cores taken from the riverbed. The resulting K values are in the range of 1.7E-3 to 1.2E-2 m/s (geometric mean: 3.72E-3 m/s).

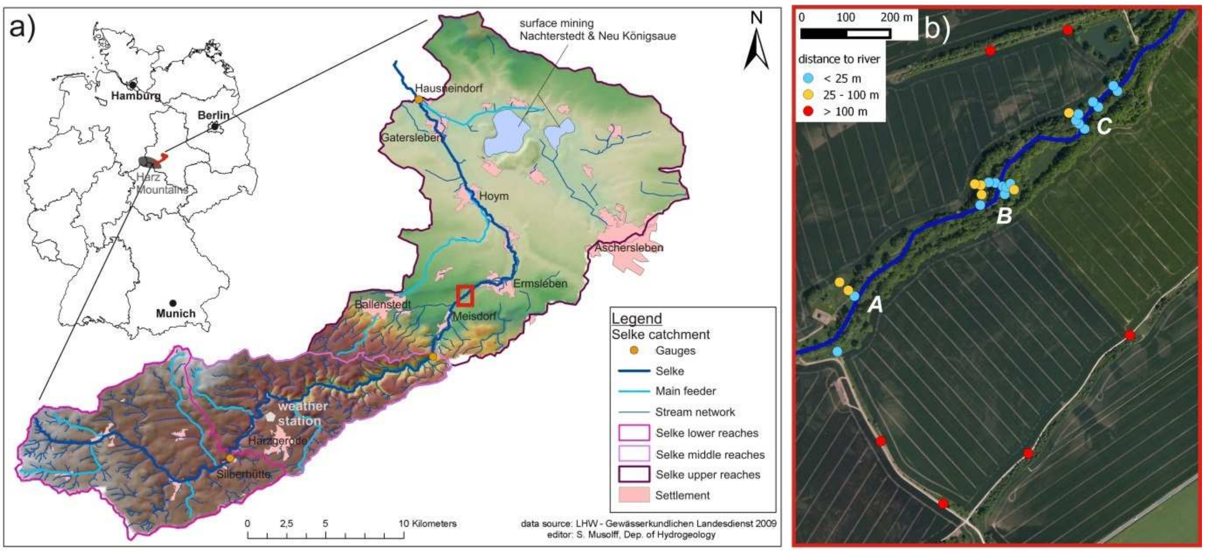

Figure 1: a) Location of the field site in the Selke river catchment in central Germany. b) Detailed aerial view of the field site and the groundwater monitoring wells. Their colors depict the distance to the Selke river, shown in the legend. The wells close to the river are furthermore grouped into three transects close to the river (A-B-C). River flow direction is from southwest to northeast.

2.2. Groundwater wells

In total 30 wells (GWM) with an inner diameter of 2.54 and 5.05 cm were drilled with by Direct Push Sonic-Drill Technology. The wells next to the river were screened in depths between 2 and 5 m for sampling of the shallow groundwater. The wells further away from the river were drilled to depth of up to 10 m below ground. All wells were thoroughly developed by intense pumping. The geodetic location (longitude, latitude, elevation above sea level) of the sampling points were surveyed by a differential GPS in combination with a laser tachymeter (Trimble GPS R8).

We classify the 30 wells into three distance-categories in order to characterize their spatial location in relation to the river. These categories are based on three buffer zones covering areas with i) less than 25 m distance to the river, ii) a distance of 25 to 100 m to the river and iii) a distance of more than 100 m to the river. The three zones are denoted as “GW near”, “GW intermediate”, and “GW distant” (Figure 1b).

2.3. Groundwater and river water sampling

During the sampling period, in total 596 groundwater and 94 river water samples were taken. Groundwater was sampled every four weeks from April 2014 until April 2016. A peristaltic pump was used to extract groundwater from the wells. During groundwater pumping water was continuously analyzed for DO, electrical conductivity (EC) and pH by a portable multi-parameter meter (find specifications and uncertainties on these devices in Table 1). Groundwater samples were taken when those field parameters were steady in time.

Surface water samples of the Selke River were taken as grab samples at two locations, upstream of the field site and downstream of the intensive field site. Here, field parameters were measured directly in the river water.

Both groundwater and river water samples were filtered with a 0.45 µm cellulose acetate membrane syringe filter and stored in a cool and dark place. Samples for major cations were acidified with nitric acid to prevent cation precipitation and adsorption. Analysis of the samples was conducted within 48 hours after sampling.

Groundwater levels were measured at each sampling date, before installing the pump. A LTC logger (Solinst LTC Levellogger Junior) was fixed at the riverbed at the field site and was recording river stage, temperature and electrical conductivity at 10 minute intervals, enabling a construction of a stage-discharge relationship for calculating continuous river discharge.

Meteorologic data was available from a federal weather station of the German Meteorological Service 15 km upstream of the site (Harzgerode, DWD-Station #2044).

2.4. Chemical analyses and Isotope Measurements

2.4.1. Major anions and cations, DOC

Anions (Cl^-, NO_2^-, NO_3^-, SO_4^{2-}, PO_4^{3-}) were analyzed using ion-chromatography (DX500, Dionex), while HCO_3^- (alkalinity) was measured in the field by Gran titration with a Hach digital titrator with 0.16 N H_2SO_4. Cations (Na^+, K^+, NH_4^+, Ca^{2+}, Mg^{2+}, Fe^{2+}) concentration were measured inductively-coupled plasma optical emission spectrometry (ICP-OES; Arcos; Spectro). Dissolved organic carbon was measured using a Shimadzu TOC-5050 analyzer. The uncertainties of the applied methods are listed in Table 1.

2.4.2. Stable nitrate isotopes

The isotopic signature of the NO_3^- molecule can be used to delineate different NO_3^- sources and to assess the impact of denitrifying activity on the NO_3^- pool. The N and oxygen isotope analyses of NO_3^- were conducted on a GasbenchII/delta V plus combination (Thermo) after using the denitrifier method to convert NO_3^- to N_2O, which enabled the simultaneous determination of $\delta^{15}N$ and $\delta^{18}O$ in the N_2O produced (Casciotti et al., 2002; Sigman et al., 2001). Nitrogen and oxygen isotope results are reported in delta notation ($\delta^{15}N$, $\delta^{18}O$) as part per thousand (‰) deviation relative to the standards AIR for N and VSMOW for oxygen (Eq. 1), where R is the ratio of the heavy to light isotopes (e.g. $^{15}N/^{14}N$; $^{18}O/^{16}O$).

$$\delta_X (‰) = [(R_{sample} - R_{standard}) / R_{standard}] \times 1000 \qquad \text{Eq. 1}$$

For calibration of N and oxygen isotope values, the reference NO_3^- IAEA-N3 ($\delta^{15}N$: +4.7 ‰ AIR; $\delta^{18}O$: +25.6 ‰ VSMOW), USGS32 ($\delta^{15}N$: +180 ‰ AIR; $\delta^{18}O$: +25.7 ‰ VSMOW), USGS 34 ($\delta^{15}N$: -

1.8 ‰ AIR; δ ^{18}O: -27.9 ‰ VSMOW), and USGS 35 (δ ^{15}N: +2.7 ‰ AIR; δ ^{18}O: +57.5 ‰ VSMOW) were used.

Isotopic enrichment during denitrification occurs via kinetic fractionation that can be described by a modified Rayleigh equation:

$$\delta = \delta_0 + \varepsilon \cdot \ln\left(\frac{NO_3^-}{(NO_3^-)_0}\right) \qquad \text{Eq. 2}$$

where ε is the enrichment factor, δ_0 and $(NO_3^-)_0$ describe the isotopic composition and the NO_3^- concentration of the educt, respectively, and δ and NO_3^- and are the isotopic composition and the NO_3^- concentration of the product.

Table 1: measurement errors of the used methods

Parameter	Method	Error
Temperature (T), pH, dissolved oxygen (DO)	Multi-parameter meter WTW 3430 with probes: SenTix 950, TetraCon 925, FDO 925.	T: ± 0,1 K pH: ± 0.01 DO: ± 0.5 %
Anions	ion-chromatography DX500, Dionex	< 3%
Cations	inductively-coupled plasma optical emission spectrometry (ICP-OES; Arcos; Spectro)	< 3%
Stable nitrate isotopes	Denitrifier method	N: ± 0.4 ‰ O: ± 1.6 ‰
DOC	Shimadzu TOC analyzer 5050	< 1 %

2.5. Statistical methods

2.5.1. Linear mixing model

In order to calculate the fraction of river water in the riparian groundwater, a linear mixing model was used, assuming chloride (Cl^-) as a conservative solute. Mixing occurs between two independent endmembers (Mengis et al., 1999; Pinay et al., 1998),which are in our case, the river water and the groundwater distant from the river that is not affected by infiltrating river water (in red color code in

Figure 1b). The fraction of river water in the riparian groundwater F_{Riv} in each well for each sampling date was calculated by

$$\boldsymbol{F_{Riv}} = \frac{[\boldsymbol{Cl^-}_{\boldsymbol{GW}}] - [\boldsymbol{Cl^-}_{\boldsymbol{Dist}}]}{[\boldsymbol{Cl^-}_{\boldsymbol{Riv}}] - [\boldsymbol{Cl^-}_{\boldsymbol{Dist}}]} \qquad \text{Eq. 3}$$

where $[Cl^-{}_{\mathrm{GW}}]$, $[Cl^-{}_{Riv}]$and $[Cl^-{}_{Dist}]$ are the Cl^- concentrations in the groundwater wells in-between the endmembers, in the river water and in the groundwater distant from the river, respectively.

In contrast to the conservatively transported Cl^-, NO_3^- is a reactive solute. Comparison of Cl^- with NO_3^- concentration has been a common tool in riparian studies to investigate potential removal pathways of NO_3^- (Altman and Parizek, 1995; Mengis et al., 1999; Pinay et al., 1998)). A deviation of the NO_3^- concentration from the concentration expected from the linear mixing model could be related to NO_3^- consumption or production by microbial reactions (denitrification, assimilation, nitrification) (Hill, 1996). To calculate the NO_3^- deficit or surplus, i.e. the deviation from the expected mixing concentration in each groundwater sample, first the theoretical NO_3^- concentration in the groundwater that would be expected by pure conservative mixing ($[NO_3^-{}_{mixGW}]$) can be calculated by using the calculated river water fraction from Eq. 3:

$$\left[NO_3^-{}_{mixGW}\right] = \left(\left[NO_3^-{}_{Riv}\right] - \left[NO_3^-{}_{Dist}\right]\right) \times F_{Riv} + \left[NO_3^-{}_{Dist}\right] \qquad \text{Eq. 4}$$

where $\left[NO_3^-{}_{Riv}\right]$ and $\left[NO_3^-{}_{Dist}\right]$ are the NO_3^- concentrations in the endmembers river water and groundwater distant from the river, respectively.

Subsequently, the difference between the theoretically NO_3^- concentration from Eq. 4 and the measured NO_3^- concentration in each well is calculated by

$$\Delta\left[NO_3^-{}_{GW}\right] = \left[NO_3^-{}_{mixGW}\right] - \left[NO_3^-{}_{GW}\right] \qquad \text{Eq. 5}$$

Values higher than zero indicate a net NO_3^- consumption or removal, whereas values below zero indicate a NO_3^- production. Furthermore, the NO_3^- deficit as a fraction of theoretical NO_3^- concentration can be calculated as:

$$\% \, NO_{3\;GW}^{-} = \frac{\Delta\left[NO_{3\;GW}^{-}\right]}{\left[NO_{3\;mixGW}^{-}\right]} \qquad \text{Eq. 6}$$

The method assumes that Cl^- and NO_3^- follow the same flow paths into the hydrological system. Furthermore, only data sets of Cl^- and NO_3^- concentrations (both theoretical and measured) can be used that lie between the measured concentrations of the two endmembers.

2.5.1.Statistical analysis

Correlation analysis was used to characterize the nonparametric relationships between responding ($\delta^{15}N$, DO) and predicting variables (e.g. water temperature, discharge) and among the predicting variables. Here, we used Spearman’s rank correlation as concentration and discharge data are often exhibits non-normal distributions and non-linear relations to each other (Jawitz and Mitchell, 2011). Based on the rank correlation a subset of predicting variables were used in a multivariate regression approach based on partial least squares regression (PLS, (Wold et al., 2001)). By using the covariance structure between the variables this method is robust against collinearity among predicting variables. The regression model is evaluated in terms of R^2, a ranking of predicting variables (defining the magnitude of influence) and by the coefficient of each predicting variable (defining the direction of influence). For the variable ranking, the VIP value is used (variable importance in projection): Only predicted variables with VIP above 1 are considered as important (see also (Musolff et al., 2015)). For the PLS regression variables were log-normalized, when bivariate relations showed a clear non-linear behavior. For rank correlation and PLS the software environment R was used.

3. Results

3.1. Hydraulic conditions

Discharge of the river Selke responds quickly to precipitation in the catchment and intense rain falls induce strong river discharge events (Figure 2a/b). Generally, river discharge is highest in the winter and spring season, whereas lowest discharges can be observed during late summer with base flow discharges around 0.2 m³/s. The warm season (May to October) of the year 2015 was dryer than the warm season of 2014, which is also reflected in the higher frequency of river discharge events in the year 2014. During the study period, five discharge events with peakflows exceeding 4 m³/s were observed.

Groundwater levels in the vicinity of the river are generally shallow with lowest levels during late summer, up to 2 m below ground, and highest levels during winter, 0.5 m below ground. In response to intense rain fall and river discharge events, groundwater levels respond quickly in the near and intermediate groundwater zone (Figure 2c). This variability decreases with distance from the river, and at some distance groundwater levels do not show any river-induced variations. Since depth to groundwater is different at each well location because of the land topography, we normalized groundwater levels in each well to the maximum and minimum groundwater levels, resulting in groundwater level variations between 0 and 1. The general direction of groundwater flow is parallel to the river in a north-easterly direction, with little change over the year (Figure 2d). Hydraulic head differences between river stage and groundwater levels indicate, that sections with river-water losses to the aquifer and sections with groundwater gains alternate along the studied 2 km river reach. Detailed information on the groundwater-surface water interaction is provided by the linear mixing model in 3.5.

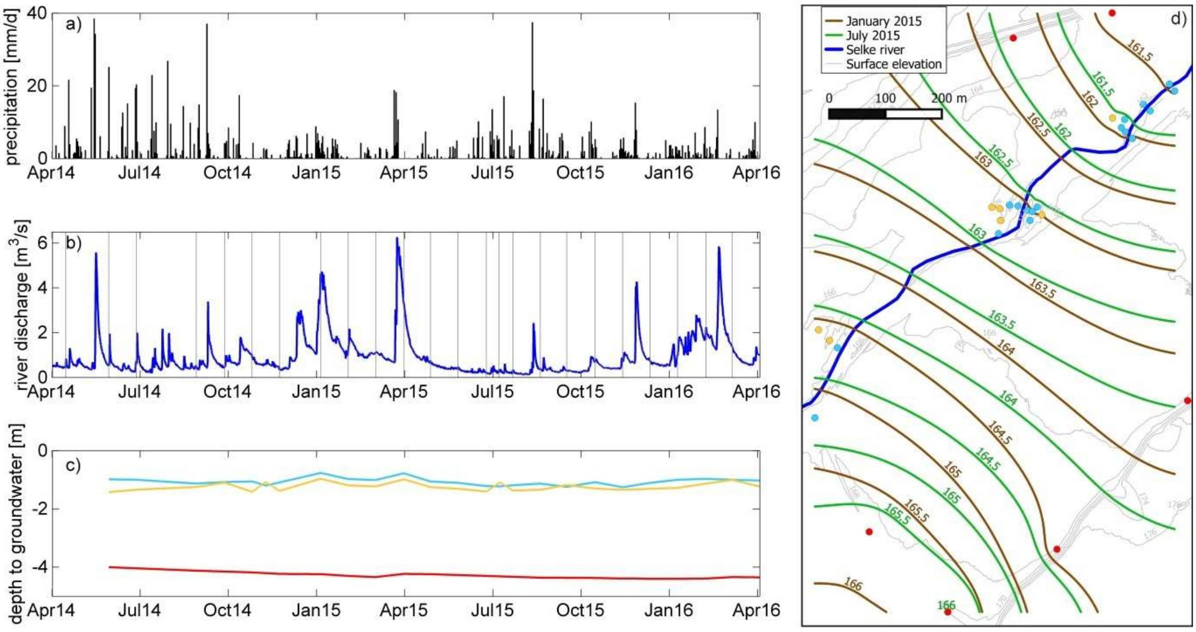

Figure 2: a) precipitation 15 km upstream of the field site within the Selke catchment (weather station Harzgerode), b) Selke river discharge (blue) and sampling dates (grey vertical lines), c) average depth to groundwater below surface over time for each groundwater zone, d) interpolated groundwater elevations above sea level at two individual sampling dates during winter (brown) and summer (green).

3.2. Spatio-temporal variation of physicochemical parameters

River temperature and river discharge are negatively related at the field site (see supporting information Figure S1a) due to seasonal variations in temperature, evapotranspiration and precipitation. The seasonal variation in temperature, can also be observed in the groundwater, but the amplitude is dampened and lagged with increasing distance from the river (Figure 3a). However, mean temperatures are similar between river water and near groundwater and only increase slightly with increasing distance from the river (Table 2). In 2015 the warm season was on average warmer than the warm season of 2014 indicated by an average river water temperature of 13.16 °C of 2014 compared to 14.05 °C during 2015.

Dissolved oxygen concentration in river water is commonly at saturation, but varies over the year due to temperature dependent solubility of oxygen in water and hence, DO is lowest during summer (Figure 3b). This inverse relation of DO and temperature is also visible in the near groundwater and the intermediate groundwater, but shows only a slight variation in the more distant groundwater

(Figure 3b). Beside this seasonal signal, DO increases with distance from the river, from < 2 mg/L next to the river during summer, to up to 9 mg/L in the groundwater distant from the river (Table 2). However, as the mean temperatures in river water and groundwater are similar, the decreased DO in the near-river groundwater cannot be explained by the temperature dependent solubility of oxygen in the river water and is presumably consumed by aerobic reactions.

The measured pH of the samples did not show a significant temporal variation. River water was generally at pH 8 while all groundwater samples show a slightly lower pH of around 7, independent of the distance from river (Figure 3c, Table 2).

3.3. Spatio-temporal variation of chloride, NO_3^- and DOC concentrations

Mean values of Cl^- and NO_3^- in river and groundwater indicate a general increase in concentration from the river towards the distant groundwater (Figure 3d/e, Table 2). In the river water samples, a clear relationship between river discharge, Cl^- and NO_3^- concentrations can be observed: For Cl^-, the concentration decreases with increasing discharge, due to dilution (see supporting information Figure S1b). In contrast, NO_3^- concentration increases with discharge (Figure S1c). Since the highest base flow discharges occur during the cold season (November to April) and also because most of the discharge events occur during late winter and spring, the Cl^- concentration is lowest during winter, whereas NO_3^- is lowest during summer (Figure 3d/e). These variations in Cl^- and NO_3^- are also visible in the groundwater next to the river but diminish with increasing distance from the river (Figure 3d/e).

DOC concentrations are highest in river water compared to the groundwater concentrations (Table 2). Variability of DOC concentrations is lower in groundwater compared to the river water. Similar to the NO_3^- concentration, DOC in river water increases with discharge (Figure S1d) and is highest during the cold season (Figure 3f).

Table 2: Mean and standard deviation (STD) of the parameters measured in river water and the three zones of groundwater

Parameter	**river water** **Mean ± STD**	**GW near** **Mean ± STD**	**GW intermediate** **Mean ± STD**	**GW distant** **Mean ± STD**
temperature [°C]	9.68 ± 4.82	9.45 ± 3.63	9.86 ± 2.54	10.35 ± 1.71
DO [mg/L]	11.15 ± 1.83	2.61 ± 2.36	3.4 ± 1.81	7.13 ± 2.09
pH [-]	7.99 ± 0.26	6.97 ± 0.26	6.84 ± 0.44	6.88 ± 0.17
Cl^- [mg/L]	32.45 ± 6.36	35.73 ± 8.93	48.98 ± 13.34	67.23 ± 24.37
NO_3^-[mgl/L]	7.41 ± 4.69	8.48 ± 4.94	15.28 ± 10.36	65.3 ± 36.49
DOC [mg/L]	3.9 ± 0.86	2.04 ± 0.64	1.82 ± 0.7	1.67 ± 0.86

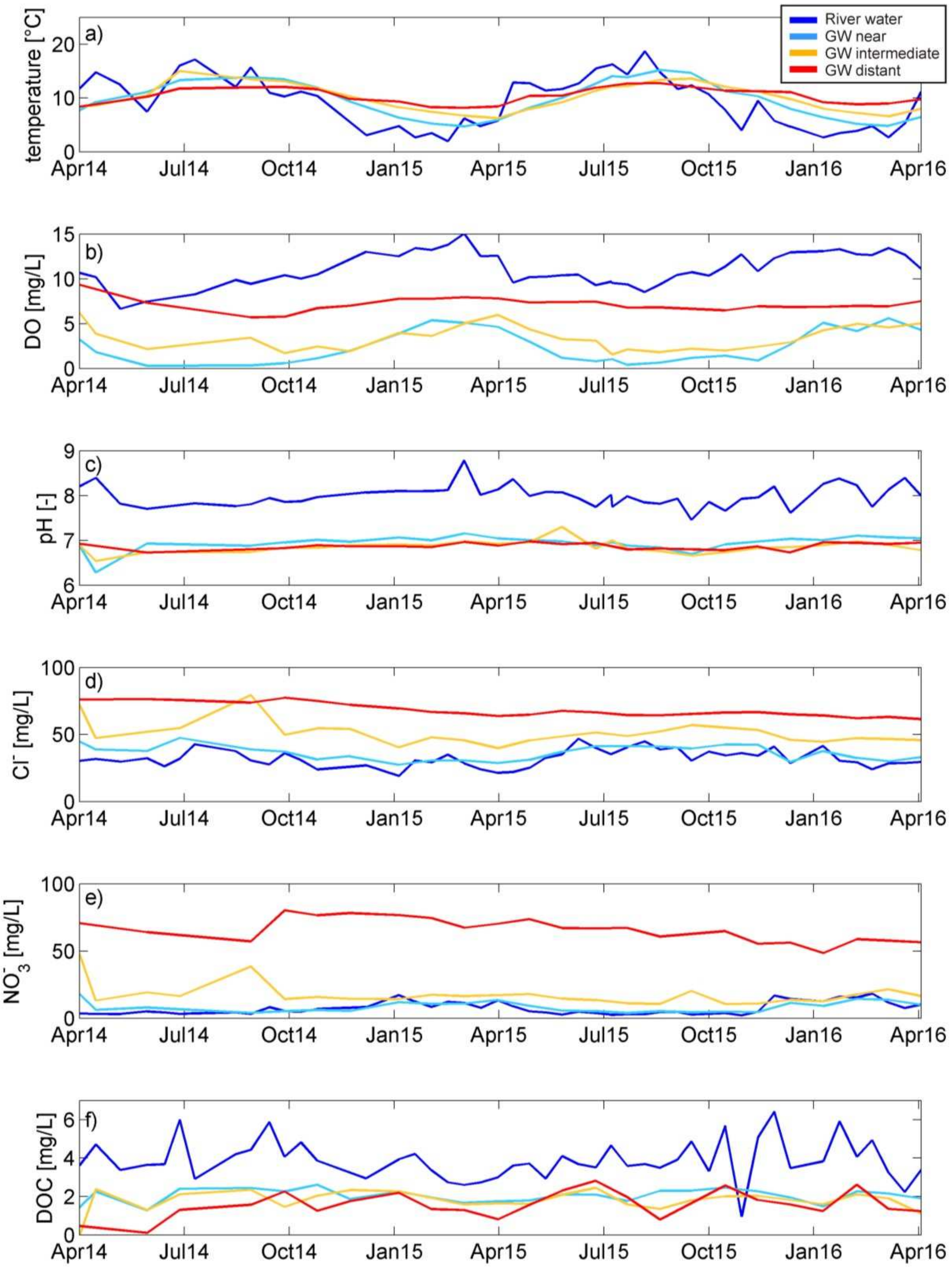

Figure 3: Physicochemical parameters over time measured in the field: a) temperature, b) dissolved oxygen (DO) and c) pH, and concentrations of d) chloride, e) NO_3^- and f) dissolved organic carbon (DOC). Number of wells in near groundwater (light blue): 17; in intermediate groundwater (orange): 8; in distant groundwater (red): 6.

3.4. Isotopic signature of the NO_3^- molecule

In general, highest $\delta^{15}N$ and $\delta^{18}O$ values in the NO_3^- molecule occur in the near and intermediate groundwater zone during the warm season (Figure 4a/b). In contrast, the distant groundwater shows a constant and unenriched isotopic signature. Also, river water has very low δ^{15}N and δ^{18}O values, but shows a moderate enrichment during the warm season. In river water and both in the near and intermediate groundwater a higher enrichment of δ^{15}N and δ^{18}O can be observed during the warm season of the year 2015, compared to the year 2014 where average air and river water temperatures were lower.

The dual fractionation factor of δ^{18}O / δ^{15}N is 0.87 (R^2=0.80) for all groundwater samples in the near zone and 0.95 (R^2=0.77) in the intermediate zone (Figure 4c). These factors are in the range of observed dual fractionation factors that indicate denitrification activity (Kendall and McDonnell, 1998) and have been observed in the many studies using NO_3^- isotopic signatures (Aravena and Robertson, 1998; Böttcher et al., 1990, 1990; Cey et al., 1999; Fukada et al., 2003; Mengis et al., 1999; Peter et al., 2012).

For the river water samples and each single well the field based, apparent enrichment factors were derived using equation Eq. 2.

The apparent N-isotope enrichment factors are in the range of -14.5 to -2.0 ‰ in the near groundwater and -6.1 to -0.73‰ in the intermediate zone. A reliable prediction of the actual enrichment factors at the field site is not possible without a proper experimental calibration by column or batch experiments. However, N-isotope enrichment factors for denitrification by groundwater denitrifying bacteria under controlled laboratory conditions have been reported to be in the range of -20 to -15 ‰ (Böttcher et al., 1990; Knöller et al., 2011). As the highest observed apparent enrichment factor at the field site of -14.5 ‰ is within that proposed range, we assume that it may represent denitrification without much interference of secondary processes. Any deviation of the observed apparent enrichment factors from this value indicates that additional processes such as mixing, nitrification, and N-assimilation by plants influence the isotopic signature (Kendall and McDonnell, 1998; Mariotti et al., 1988).

The observed apparent enrichment factor in the distant groundwater of around -1 ‰ indicates that denitrification does not have a significant impact here. However, in the river water, small apparent enrichment factors were observed, presumably related to the inflow of denitrified groundwater into the river.

Isotopic data of the groundwater shows no evidence of intense nitrification (the production of NO_3^- by microbial oxidation of reduced inorganic N), which would lead to depleted $\delta^{15}N$ values (Kendall and McDonnell, 1998) . The mineralization of organic N from decaying plants and the subsequent nitrification may add an amount of NO_3^- comparable to catchments not affected by agricultural land use. A higher extent of nitrification can be expected in the unsaturated zone below the agricultural fields, because here inorganic reduced N originating from manure and fertilizer can be oxidized to NO_3^- (Choi and Ro, 2003; Cook and Herczeg, 2000; Kendall and McDonnell, 1998), which in turn can act as the NO_3^- end-member when reaching the saturated zone in the distant groundwater.

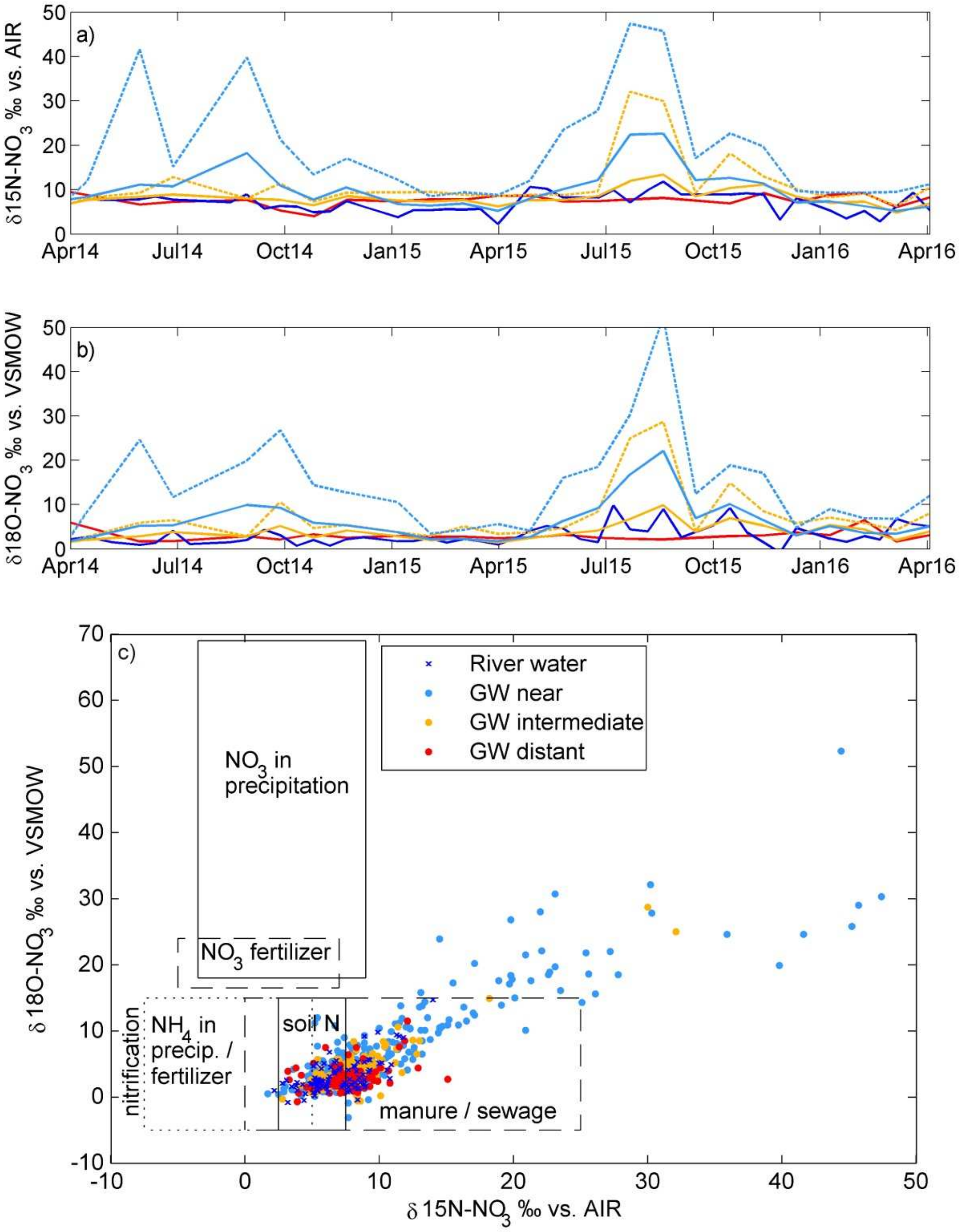

Figure 4: a) mean δ^{15}N and b) mean δ^{18}O over time for each groundwater zone and the river water, dashed lines of the near and the intermediate zone indicate the maximum values c) Dual isotope plot of the δ^{15}N and δ^{18}O composition of NO$_3^-$ (after Kendall and McDonnel (1998)).

3.5. River water fractions in groundwater and NO_3^- deficit calculations based on mixing model

For 73 % of all groundwater samples the mixing model was applicable. The rest of the samples were excluded because here, Cl^- was temporally lower in the groundwater than in the river water (see section 2.5.1).

In general, the fraction of river water in the groundwater suggests, that river water is lost to the southern riparian zone across the entire river length of our field site (Figure 5a). In contrast, the low river water fractions and elevated Cl^- concentrations observed at the northern transect “A” suggest that here the river is gaining groundwater from the northern bank at this location. In the northern part of the meander shaped site at transect “B”, the flow conditions are alternating from losing to gaining conditions, depending on the proximity of the well to the river. Those alternating river-groundwater exchange conditions are closely linked to the N isotope signatures and the magnitude of the apparent enrichment factors: The higher the river water fraction, the higher is the $\delta^{15}N$ value and also the magnitude of the apparent enrichment factors (Figure 5a/b/c). For example at transect “C” the river is strongly losing water to the aquifer on both sides, leading to very high river water fractions in the groundwater and concurrently show highest $\delta^{15}N$ values and highest magnitudes of apparent enrichment factors. In contrast, at sites where the river is gaining groundwater, the lowest $\delta^{15}N$ and lowest magnitudes of apparent enrichment factors can be observed.

The theoretical NO_3^- concentrations that would be expected by pure conservative mixing ($[NO_3^-{}_{mixGW}]$, Eq. 4) are given in Figure 6a. A strong NO_3^- deficit is visible, for the bulk of the samples in both the near and the intermediate groundwater. Nevertheless, for some sampling points, a slight enrichment in NO_3^- concentrations was calculated, especially for low NO_3^- concentrations, which could indicate some nitrification activity. However, due to the fact that neither the isotopic data show signs of and the fact that ammonia concentrations were most of the time too low to be detected in groundwater, it is unlikely that nitrification is of great importance at our field site.

In general, the absolute values of the NO_3^- concentrations and the NO_3^- deficits are larger in the intermediate groundwater zone, than in the near groundwater. Furthermore, the deficit is larger during the warm season than during the cold season, again depicting a strong seasonal effect.

The $\delta^{15}N$ values show an increasing enrichment with increasing NO_3^- deficit calculated by the mixing model for both groundwater in near and intermediate distance from the river (Figure 6b). However, correlation between the data derived by the two different methods is only on a fair level. Please note, that for the fit with an R^2 of 0.37 the three samples with $\delta^{15}N$ values above 25 (hollow circles in Figure 6b) were excluded. If these three data points of extraordinary $\delta^{15}N$ enrichment taken during the late summer 2015, are included goodness of fit is lower at $R^2 = 0.20$.

The reason for the deviation between the NO_3^- deficit calculated by the mixing model and the $\delta^{15}N$ enrichment may be due to other processes besides denitrification, such as N assimilation by plants or ANAMMOX (Burgin and Hamilton, 2007; Canfield et al., 2010) which may lead to subordinated N-depletion in the riparian zone compared to denitrification (Naeher et al., 2015; Wang et al., 2012).

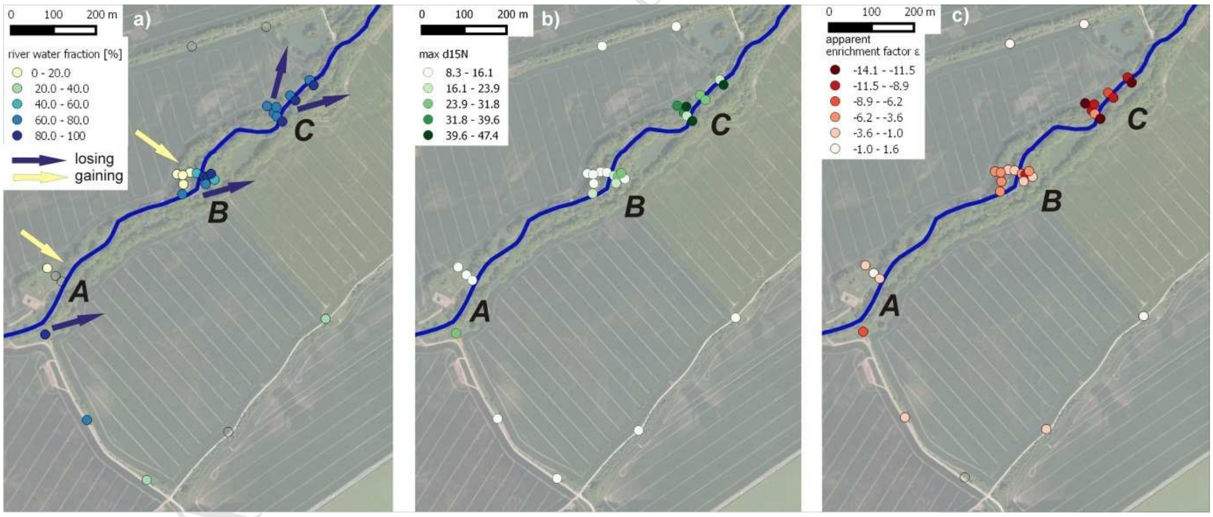

Figure 5: a) Mean river water fraction calculated by Eq. 3 in the groundwater calculated from the mixing model. Arrows are showing the local direction of groundwater-river exchange (losing or gaining). b) Maximum $\delta^{15}N$ values for each well c) apparent enrichment factors derived by Eq. 2

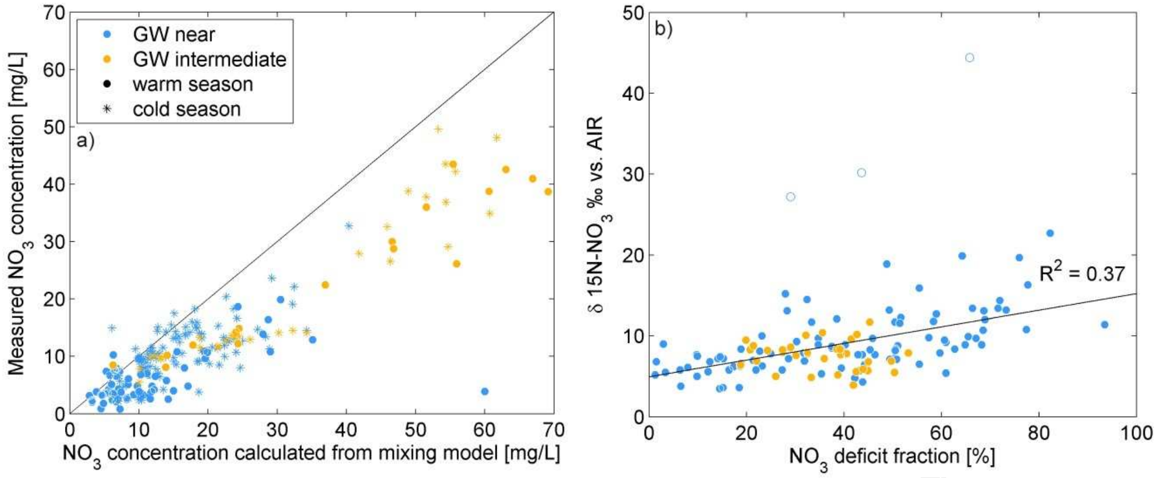

Figure 6: a) Measured NO$_3^-$ concentrations versus calculated theoretical NO$_3^-$ concentration based on mixing model for near and intermediate groundwater samples during summer and winter period. The black line represents the 1:1 line. b) Comparison between NO$_3^-$ deficit fraction and δ^{15}N composition. The black line represents a linear fit through all data points of both near and intermediate groundwater. Hollow circles in b) are excluded from the linear fit.

3.6. Correlation analysis and PLS model results

Lowest DO and highest δ^{15}N compositions can be found primarily in the near and intermediate groundwater when temperature is higher than approximately 10°C (Figure 3a/b, Figure 4a and Figure 7a/b). In the river near groundwater the enrichment of δ^{15}N is directly related to anaerobic conditions (Figure 7c) which are required for denitrification. In contrast, similar temperatures in the distant groundwater did not affect DO and δ^{15}N greatly and δ^{15}N composition is insensitive to DO concentration. Thus, the proximity to the river is an additional important factor that controls both aerobic respiration and denitrification. The fraction of river water in the groundwater (F_{Riv}), calculated by the linear mixing model provides additional: The strongly enriched δ^{15}N isotopic signatures mostly occur when F_{Riv} is high (Figure 7d). During high river discharges the enrichment of δ^{15}N is lower (Figure 7e). This is in line with the slight negative relationship between groundwater levels and the δ^{15}N enrichment, indicating that under high groundwater levels the δ^{15}N enrichment is less intense (Figure 7f).

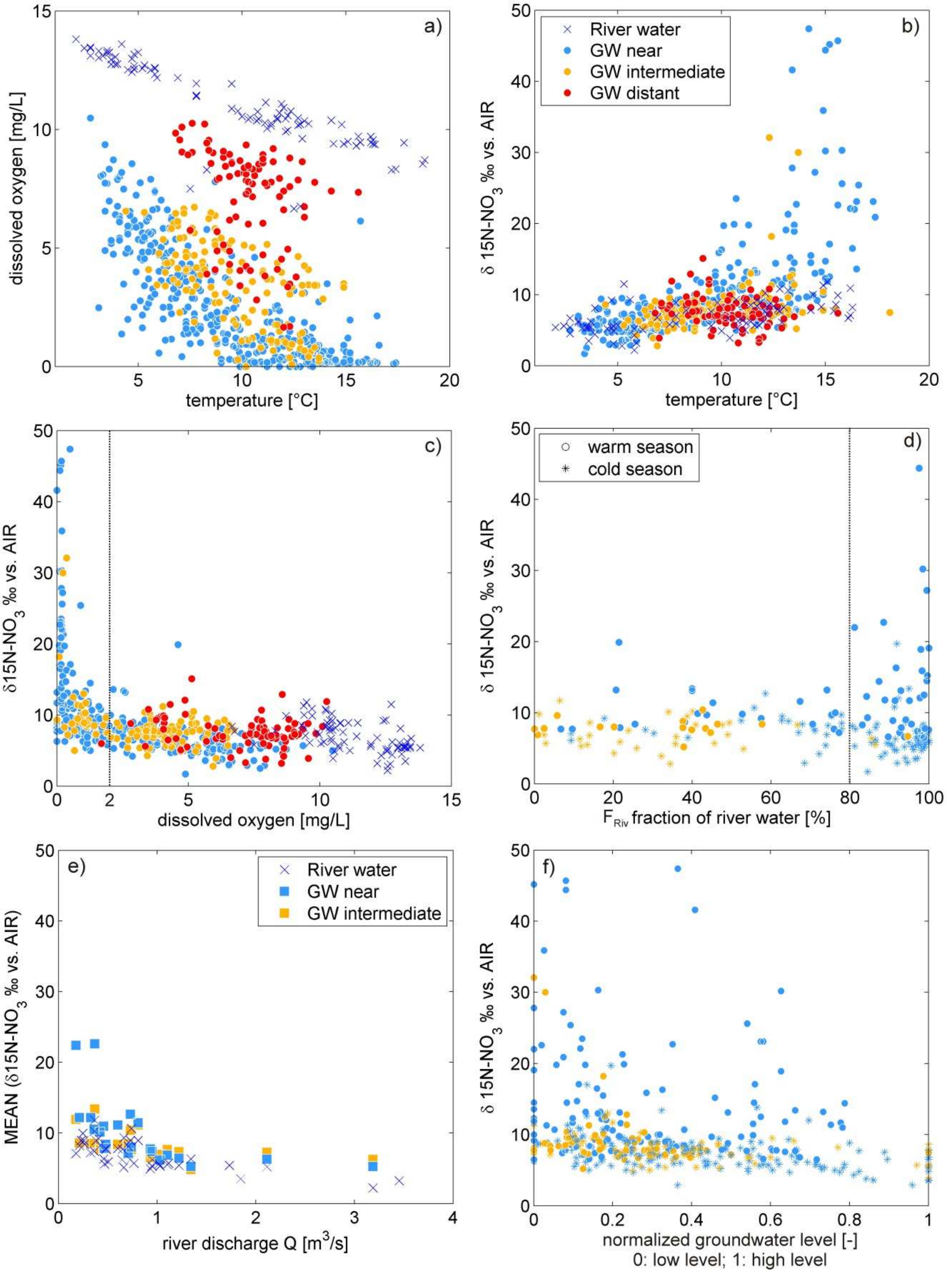

Figure 7: a) Water temperature vs. dissolved oxygen (DO) and b) vs. δ^{15}N composition of NO_3^-, c) dissolved oxygen (DO) vs. δ^{15}N composition of NO_3^- , d) calculated fraction of river water (F_{Riv}) in groundwater based on the linear mixing model vs. δ^{15}N composition, e) river discharge at sampling time vs. δ^{15}N composition of river water and mean δ^{15}N values of near and intermediate groundwater f) normalized groundwater levels vs. δ^{15}N composition.

Spearman’s rank correlation (Table 3) reveals that the dynamics of DO and of $\delta^{15}N$ are negatively correlated with each other (r_{spear} = -0.59) and show strong similarities with a set of other variables as well. For DO, groundwater NO_3^- concentrations (positive), water temperature (negative) and discharge (positive) are most important ($r_{spear} \geq 0.5$). We also note weak correlations (r_{spear} 0.3-0.5) with distance of the well from the river (positive), Eh (positive), potassium (K) (negative) and normalized groundwater levels (positive). For $\delta^{15}N$, groundwater temperature (positive), river discharge (negative) and groundwater NO_3^- concentrations (negative) are most important. Weaker correlations were found with potassium (positive), normalized groundwater level (negative) and pH (negative).

	DO	distance to river	river Q	norm. GWL	GW temp.	EC	pH	Eh	Ca^{2+}	Mg^{2+}	Na^+	K^+	SO_4^{2-}	HCO_3^-	Cl^-	Fe^{2+}	PO_4^{3-}	DOC	NO_2^-	NH_4^+	NO_3^-	F_{Riv}	apparent ε	$\delta^{15}N$
DO	1.00																							
distance to river	**0.45**	1.00																						
river Q	**0.49**	0.00	1.00																					
norm. GWL	**0.32**	-0.04	0.58	1.00																				
GW temperature	**-0.56**	0.10	-0.73	-0.48	1.00																			
EC	0.10	0.58	-0.22	-0.23	0.35	1.00																		
pH	0.24	-0.28	0.37	0.21	-0.51	-0.43	1.00																	
Eh	**0.35**	0.13	0.52	0.33	-0.42	0.03	0.14	1.00																
Ca^{2+}	0.07	0.56	-0.20	-0.20	0.37	0.97	-0.45	0.08	1.00															
Mg^{2+}	0.12	0.62	-0.24	-0.23	0.41	0.95	-0.48	0.01	0.93	1.00														
Na^+	0.02	0.50	-0.32	-0.27	0.51	0.90	-0.44	-0.04	0.91	0.90	1.00													
K^+	**-0.32**	0.15	-0.46	-0.33	0.64	0.61	-0.46	-0.18	0.66	0.60	0.77	1.00												
SO_4^{2-}	0.00	0.49	-0.22	-0.22	0.33	0.91	-0.50	0.12	0.94	0.84	0.81	0.65	1.00											
HCO_3^-	0.04	0.57	-0.27	-0.26	0.48	0.91	-0.45	-0.04	0.90	0.93	0.89	0.63	0.79	1.00										
Cl^-	0.12	0.58	-0.26	-0.27	0.43	0.93	-0.45	-0.04	0.90	0.93	0.91	0.60	0.81	0.91	1.00									
Fe^{2+}	0.00	0.08	0.28	-0.18	0.05	-0.04	-0.07	0.15	-0.08	0.05	-0.11	-0.17	-0.08	0.00	0.05	1.00								
PO_4^{3-}	0.09	0.15	-0.10	-0.11	0.00	0.13	0.05	0.05	0.15	0.15	0.09	0.08	0.12	0.20	0.07	-0.24	1.00							
DOC	-0.19	-0.22	-0.08	-0.04	0.16	-0.06	0.10	-0.13	-0.03	-0.07	-0.01	0.15	-0.07	-0.02	-0.05	-0.19	0.01	1.00						
NO_2^-	-0.13	0.24	-0.16	-0.11	0.28	0.06	-0.33	-0.53	0.15	0.18	0.17	0.16	0.14	0.20	0.16	-0.50	0.03	0.43	1.00					
NH_4^+	0.00	-0.08	0.00	0.09	-0.27	-0.17	0.05	0.27	-0.16	-0.08	-0.20	-0.17	-0.09	-0.15	-0.14	-0.08	0.31	0.10	0.59	1.00				
NO_3^-	**0.71**	0.59	0.38	0.23	-0.36	0.49	0.01	0.29	0.47	0.51	0.33	-0.09	0.37	0.41	0.44	0.08	0.16	-0.17	0.26	0.11	1.00			
F_{Riv}	-0.18	-0.51	-0.02	0.07	-0.17	-0.61	0.35	-0.20	-0.63	-0.59	-0.55	-0.31	-0.62	-0.58	-0.57	-0.39	-0.13	0.07	-0.11	0.05	-0.40	1.00		
apparent ε	0.19	0.30	0.00	-0.09	0.09	0.69	-0.29	0.27	0.68	0.65	0.59	0.49	0.68	0.64	0.62	0.08	0.14	0.04	0.36	0.03	0.44	-0.51	1.00	
$\delta^{15}N$	**-0.59**	-0.13	**-0.52**	**-0.37**	**0.59**	0.19	**-0.34**	**-0.27**	0.18	0.20	0.25	**0.43**	0.21	0.27	0.22	-0.25	0.01	0.18	-0.18	-0.02	**-0.50**	-0.03	0.02	1.00

Table 3: Spearman’s rank correlation matrix between measured and derived variables. Dark colors indicate higher absolute correlations. Green indicates negative, blue positive correlations. “Distance to river” stands for the shortest distance between well and river, “river Q” is the river discharge during the sampling time, “norm GWL” means the normalized groundwater level as described in section 3.1 , “F_{Riv}.” stands for the fraction of river water in the groundwater.

To investigate the effect of proximity to the river in more detail, we put only those groundwater samples into a partial least square (PLS) regression model, where river water was above 80% (please find further information to that threshold in the Supporting Information (Figure S2). For the PLS regression, groundwater temperature, river discharge, normalized groundwater heads and pH were taken as predictors, DO and $\delta^{15}N$ as responding variables. The model explained 68.3 % of DO variance and 67.2 % of $\delta^{15}N$ variance. Groundwater temperature only was identified as the most important predictor with a variable importance in prediction (VIP) of > 1 (see Table 4). Although river discharge and groundwater temperature are correlated to each other ($r_{spear} = -0.73$, Table 3), the PLS model reveals that groundwater temperature is the dominant control of DO and $\delta^{15}N$. Groundwater temperature alone can explain 67.8% of the variance in DO and 66.2% of the variance in $\delta^{15}N$ using a simple exponential model in the groundwater samples with a river water fraction of more than 80%.

Table 4: PLS model regression parameters and results for the prediction of dissolved oxygen (DO) and $\delta^{15}N$. Only samples with a river water fraction F_{Riv}> 80% were taken into account (n=116). VIP (variable importance in prediction), coeff (coefficient) defining the direction of influence on responding variable. Variables marked with an asterisk were log-normalized prior to analysis.

	DO*		$\delta^{15}N$*	
	VIP	**coeff**	**VIP**	**coeff**
Groundwater temperature	1.97	-0.30	1.96	0.12
River discharge*	0.34	-0.13	0.36	-0.02
pH	0.12	-0.11	0.05	0.00
normalized groundwater level	0.08	-0.04	0.09	-0.01
R^2	0.683		0.672	

4. Discussion

4.1. Key controlling factors for NO_3^- removal

Our results suggest an increase of denitrification activity with a growing influence of infiltrating river water on the riparian groundwater, but with temperature as a key constraint. The strong temperature effect on both DO concentration and denitrification has frequently been observed in other studies (Bu et al., 2017; Clément et al., 2003; Dhondt et al., 2003; Diem et al., 2013a; Peter et al., 2012; Vieweg et al., 2016). Low DO concentrations are presumably caused by intense heterotrophic aerobic respiration caused by a river-borne carbon source (Diem et al., 2013a) and secondly by high temperature during the warm season. In turn, $\delta^{15}N$ composition increases with decreasing DO concentration (Figure 7e) which is related to the inhibition effect of DO on anaerobic heterotrophic denitrification (Rivett et al., 2008; Vidon and Hill, 2004a). Many studies have reported a threshold in DO concentration of around 2 mg/L, below which denitrification activity strongly increases (see review of (Rivett et al., 2008)), which is in line with our results (Figure 7c).

We found, that at losing river sections, the highest $\delta^{15}N$ values and apparent enrichment factors match the highest river water fractions in the groundwater (Figure 5). These results clearly indicate that i) denitrification activity is highest at losing river sections as indicated by significantly elevated $\delta^{15}N$ values, and ii) at losing river sections, our calculated apparent enrichment factors are close to the enrichment factors observed for denitrifying bacteria than at gaining sections. This indicates that at losing river sections denitrification is the major process for NO_3^- depletion.

This positive effect of river proximity on denitrification activity in groundwater has also been observed in other studies (Addy et al., 2002; Devito et al., 2000; Mayer et al., 2007; Ostrom et al., 2002). They hypothesized that this effect was related to the generally higher organic carbon content in the near riparian aquifer compared to the groundwater at increasing distance from the river. At our field site, this hypothesis can be further corroborated by the strong depletion of DO by heterotrophic aerobic respiration of bioavailable carbon from the river in the near-stream groundwater zone. However, further clarification of the potential relationship between bioavailable carbon and denitrification activity is difficult on the basis of our bulk DOC concentration data, which does not capture the bioavailability of carbon sources in the riparian zone (Brugger et al., 2001; Brunke and Gonser, 1997; Hedin et al., 1998; Leenheer and Croué, 2003). Furthermore, the carbon may also be exposed to a potential consumption by aerobic respiration at an unknown rate.

For an improved evaluation of the relationship between carbon quality and denitrification carbon quality could be analyzed using methods such as PARAFAC (Eimers et al., 2008; Kothawala et al., 2015) and isotopic signature of ^{13}C in the dissolved *in*organic carbon , which decreases during heterotrophic denitrification (Aravena and Robertson, 1998; Hosono et al., 2015; Lambert et al., 2011).

4.2. Effects of river discharge and groundwater level

Based on the PLS-model, we observe a weak negative influence of river discharge on DO depletion as well as of river discharge on enrichment of δ^{15}N (Table 4, Figure 7e). This suggests that reactive activity is lower during high discharges. This is in line with previous studies (Ostrom et al., 2002; Peter et al., 2012), where this effect was attributed to the higher groundwater flow velocities during events, leading to a shorter contact time to the sediment containing aerobic and anaerobic bacteria (Findlay, 1995; Peter et al., 2012; Valett et al., 1996). Our data is in line with this hypothesis, as the magnitude of hydraulic gradients between river and groundwater show a negative effect on δ^{15}N enrichment. We argue that an additional mobilization of carbon during events that may fuel aerobic respiration and denitrification is of only minor importance. Although a significant mobilization of carbon occurs during events (Eimers et al., 2008; Fasching et al., 2015; Meybeck, 1982; Musolff et al., 2015) it does not necessarily contain a higher content of bioavailable carbon consisting of lower molecular weights like amino acids and organic acids (Raeke et al., 2017).

Interestingly, the PLS model further reveals that besides river discharge, groundwater levels also show a slightly negative correlation with δ^{15}N enrichment (Table 4, Figure 7f). This is in contrast to several other studies, which have suggested that during high groundwater levels additional carbon and NO_3^- sources may be mobilized by groundwater tapping into upper soil layers (Biron et al., 1999; Creed et al., 1996; Hill et al., 2000) which can result in increased denitrification activities (Burt et al., 2002;

Gift et al., 2010; Hefting et al., 2004; Simmons et al., 1992). However, groundwater level fluctuations at our field site in the near and intermediate groundwater zone are relatively small (< 0.6 m) and thus, additional mobilization of solutes from the upper soil layer is limited.

4.3. Nitrate removal potential of the riparian zone

The fraction of NO_3^- removed from the mass reflected in the initial NO_3^- concentration for each well in the near and the intermediate zone was calculated based on the linear mixing model (Figure 8a, section 2.5.1) and the isotopic composition combined with the apparent enrichment factor (re-arranging Eq. 2) (Figure 8b, section 3.4). A strong seasonality can be observed over time, especially for the calculated NO_3^- deficit fraction by the linear mixing model (Figure 8a). Here, the highest fractions of removal occur during the summer months (July to October) and in the near groundwater with varying NO_3^- removal fractions between 15 % and 75 %. In the intermediate zone, only 20 % to 45 % variation can be observed. In estimates of NO_3^- removal based on the isotopic data, this seasonality is less evident. However, highest NO_3^- removal fractions were also observed in the months July and August in 2015. The lower removal fractions during the year 2014 can be explained by the lower $\delta^{15}N$ values during this time period (Figure 4a). Furthermore, compared to the linear mixing model results, the isotopic method yields generally higher removal fractions for the intermediate zone, which at certain times were higher than in the near groundwater zone. Both methods yield removal fractions that are on the order of NO_3^- removal fractions found by other studies e.g. (Cooper, 1990; Puckett and Hughes, 2005).

Average NO_3^- removal rates over the entire period of in the near and the intermediate groundwater zone were on the order of 1.0 mg-N/L/d and 3.1 mg-N/L/d, respectively. These values indicate that in the intermediate zone the absolute amount of NO_3^- being removed is about three times higher than in the near groundwater zone, whereas the percentage of removal is slightly lower in the intermediate zone, which is related to the higher NO_3^-concentrations in the intermediate groundwater. These values are within the large range of observed denitrification rates for riparian zones (Addy et al., 2002; Baker and Vervier, 2004; Kellogg et al., 2005). We emphasize, that based on our mixing model, the NO_3^- which is consumed in the near GW zone consists of only 20 % NO_3^- (0.2 mg-N/L/d) originating from the distant GW. Conversely, in the intermediate GW zone 60 % of the denitrified NO_3^- (1.9 mg-N/L/d) originate from the distant GW. Therefore, the intermediate GW zone is more important in terms of the absolute rate of removal of groundwater borne NO_3^-, compared to the near groundwater zone, where mainly river borne NO_3^- is removed.

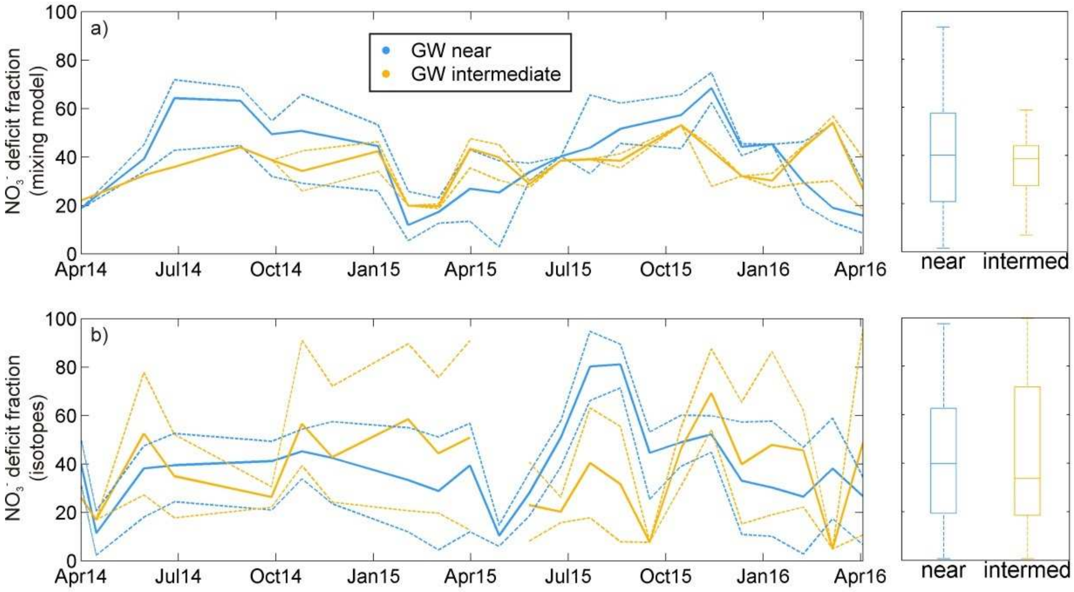

Figure 8: a) Nitrate deficit calculated by the linear mixing model over the sampling period for the groundwater samples next to the river and with an intermediate distance to the river. b) Denitrified fraction of NO_3^- based on the calculated apparent enrichment factors. Dashed lines show the 25 and 75-Quantiles.

5. Conclusions

River and groundwater hydrological, hydrochemical and isotopic data from a four-weekly sampling campaign over a two year period were statistically evaluated to quantitatively rank the factors that control NO_3^- concentrations and denitrification efficiency in the riparian zone.

Close to the river, groundwater hydraulics and hydrochemistry are strongly affected by river water infiltration. Here, consumption of DO and the enrichment of $\delta^{15}N$ and $\delta^{18}O$ of the NO_3^- molecule provide evidence for denitrification, especially during the late summer months. In groundwater with a river water fraction larger than 80%, temperature can explain 67.8% of the variance in DO and 66.2% of the variance in $\delta^{15}N$ using a simple exponential model. These high river water fractions occur at locations where river water infiltrates into the riparian aquifer (losing conditions), which presumably is a key driver for the supply of bioavailable carbon fueling microbial activity.

On average, we estimated a NO_3^- depletion on the order of 40 % of the NO_3^- concentration in the riparian aquifer within a zone of 100 m from the river. In contrast to other studies, our data suggests, that hydrological factors that have been linked to an increased mobilization of carbon sources, e.g. during high river discharges or high groundwater levels play a minor role for both consumption of DO and denitrification.

Expanding on previous research on denitrification in riparian zones, our study emphasizes that besides temperature, the interactions between river and groundwater and the resulting water and solute fluxes play a crucial role in controlling reaction rates. This knowledge could provide valuable guidance for the design of river restoration measures, which should ensure high connectivity between river and groundwater to maximize denitrification potentials.

6. Acknowledgments

For the drilling works we thank Simon Kögler, Helko Kotas, and Andreas Schoßland. We highly acknowledge Oliver Bednorz for carrying out the river and groundwater sampling. For the laboratory work we would like to thank Martina Neuber, Sybille Mothes, Jürgen Steffen and Simone Puschendorf. We thank the editor and two anonymous reviewers for their thoughtful comments to improve the quality of the manuscript.

7. Literature

Addy, K., Kellogg, D.Q., Gold, A.J., Groffman, P.M., Ferendo, G., Sawyer, C., 2002. In situ push–pull method to determine ground water denitrification in riparian zones. J. Environ. Qual. 31, 1017–1024.

Altman, S.J., Parizek, R.R., 1995. Dilution of Nonpoint-Source Nitrate in Groundwater. J. Environ. Qual. 24, 707–718. https://doi.org/10.2134/jeq1995.00472425002400040023x

Aravena, R., Robertson, W.D., 1998. Use of Multiple Isotope Tracers to Evaluate Denitrification in Ground Water: Study of Nitrate from a Large-Flux Septic System Plume. Ground Water 36, 975–982. https://doi.org/10.1111/j.1745-6584.1998.tb02104.x

Bachmann, G.H., Ehling, B.C., Eichner, R., Schwab, M., 2008. Geologie von Sachsen-Anhalt, 1st ed. Schweizerbart'sche, E., Stuttgart.

Baker, M.A., Vervier, P., 2004. Hydrological variability, organic matter supply and denitrification in the Garonne River ecosystem. Freshw. Biol. 49, 181–190. https://doi.org/10.1046/j.1365-2426.2003.01175.x

Balestrini, R., Sacchi, E., Tidili, D., Delconte, C.A., Buffagni, A., 2016. Factors affecting agricultural nitrogen removal in riparian strips: Examples from groundwater-dependent ecosystems of the Po Valley (Northern Italy). Agric. Ecosyst. Environ. 221, 132–144. https://doi.org/10.1016/j.agee.2016.01.034

Biron, P.M., Roy, A.G., Courschesne, F., Hendershot, W.H., Côté, B., Fyles, J., 1999. The effects of antecedent moisture conditions on the relationship of hydrology to hydrochemistry in a small forested watershed. Hydrol. Process. 13, 1541–1555. https://doi.org/10.1002/(SICI)1099-1085(19990815)13:11<1541::AID-HYP832>3.0.CO;2-J

Böhlke, J.K., Denver, J.M., 1995. Combined Use of Groundwater Dating, Chemical, and Isotopic Analyses to Resolve the History and Fate of Nitrate Contamination in Two Agricultural Watersheds, Atlantic Coastal Plain, Maryland. Water Resour. Res. 31, 2319–2339. https://doi.org/10.1029/95WR01584

Böttcher, J., Strebel, O., Voerkelius, S., Schmidt, H.-L., 1990. Using isotope fractionation of nitrate-nitrogen and nitrate-oxygen for evaluation of microbial denitrification in a sandy aquifer. J. Hydrol. 114, 413–424. https://doi.org/10.1016/0022-1694(90)90068-9

Brugger, A., Wett, B., Kolar, I., Reitner, B., Herndl, G.J., 2001. Immobilization and bacterial utilization of dissolved organic carbon entering the riparian zone of the alpine Enns River, Austria. Aquat. Microb. Ecol. 24, 129–142. https://doi.org/10.3354/ame024129

Brunke, M., Gonser, T., 1997. The ecological significance of exchange processes between rivers and groundwater. Freshw. Biol. 37, 1–33. https://doi.org/10.1046/j.1365-2427.1997.00143.x

Burgin, A.J., Hamilton, S.K., 2007. Have we overemphasized the role of denitrification in aquatic ecosystems? A review of nitrate removal pathways. Front. Ecol. Environ. 5, 89–96. https://doi.org/10.1890/1540-9295(2007)5[89:HWOTRO]2.0.CO;2

Burt, T.P., Pinay, G., Matheson, F.E., Haycock, N.E., Butturini, A., Clement, J.C., Danielescu, S., Dowrick, D.J., Hefting, M.M., Hillbricht-Ilkowska, A., Maitre, V., 2002. Water table fluctuations in the riparian zone: comparative results from a pan-European experiment. J. Hydrol. 265, 129–148. https://doi.org/10.1016/S0022-1694(02)00102-6

Bu, X.L., Zhao, C.X., Han, F.Y., Xue, J.H., Wu, Y.B., 2017. Nitrate reduction in groundwater and isotopic investigation of denitrification in integrated tree-grass riparian buffers in Taihu Lake watershed, eastern China. J. Soil Water Conserv. 72, 45–54. https://doi.org/10.2489/jswc.72.1.45

Canfield, D.E., Glazer, A.N., Falkowski, P.G., 2010. The Evolution and Future of Earth's Nitrogen Cycle. Science 330, 192–196. https://doi.org/10.1126/science.1186120

Casciotti, K.L., Sigman, D.M., Hastings, M.G., Böhlke, J.K., Hilkert, A., 2002. Measurement of the Oxygen Isotopic Composition of Nitrate in Seawater and Freshwater Using the Denitrifier Method. Anal. Chem. 74, 4905–4912. https://doi.org/10.1021/ac020113w

Cey, E.E., Rudolph, D.L., Aravena, R., Parkin, G., 1999. Role of the riparian zone in controlling the distribution and fate of agricultural nitrogen near a small stream in southern Ontario. J. Contam. Hydrol. 37, 45–67. https://doi.org/10.1016/S0169-7722(98)00162-4

Choi, W.-J., Ro, H.-M., 2003. Differences in isotopic fractionation of nitrogen in water-saturated and unsaturated soils. Soil Biol. Biochem. 35, 483–486. https://doi.org/10.1016/S0038-0717(02)00299-7

Clément, J.-C., Holmes, R.M., Peterson, B.J., Pinay, G., 2003. Isotopic investigation of denitrification in a riparian ecosystem in western France. J. Appl. Ecol. 40, 1035–1048. https://doi.org/10.1111/j.1365-2664.2003.00854.x

Cook, P.G., Herczeg, A.L. (Eds.), 2000. Environmental Tracers in Subsurface Hydrology. Springer US, Boston, MA.

Cooper, A.B., 1990. Nitrate depletion in the riparian zone and stream channel of a small headwater catchment. Hydrobiologia 202, 13–26. https://doi.org/10.1007/BF00027089

Creed, I.F., Band, L.E., Foster, N.W., Morrison, I.K., Nicolson, J.A., Semkin, R.S., Jeffries, D.S., 1996. Regulation of Nitrate-N Release from Temperate Forests: A Test of the N Flushing Hypothesis. Water Resour. Res. 32, 3337–3354. https://doi.org/10.1029/96WR02399

Denk, T.R.A., Mohn, J., Decock, C., Lewicka-Szczebak, D., Harris, E., Butterbach-Bahl, K., Kiese, R., Wolf, B., 2017. The nitrogen cycle: A review of isotope effects and isotope modeling approaches. Soil Biol. Biochem. 105, 121–137. https://doi.org/10.1016/j.soilbio.2016.11.015

Devito, K.J., Fitzgerald, D., Hill, A.R., Aravena, R., 2000. Nitrate dynamics in relation to lithology and hydrologic flow path in a river riparian zone. J. Environ. Qual. 29, 1075–1084.

Dhondt, K., Boeckx, P., Van Cleemput, O., Hofman, G., 2003. Quantifying nitrate retention processes in a riparian buffer zone using the natural abundance of 15N in NO3−. Rapid Commun. Mass Spectrom. 17, 2597–2604. https://doi.org/10.1002/rcm.1226

Diem, S., Cirpka, O.A., Schirmer, M., 2013a. Modeling the dynamics of oxygen consumption upon riverbank filtration by a stochastic–convective approach. J. Hydrol. 505, 352–363. https://doi.org/10.1016/j.jhydrol.2013.10.015

Diem, S., Rudolf von Rohr, M., Hering, J.G., Kohler, H.-P.E., Schirmer, M., von Gunten, U., 2013b. NOM degradation during river infiltration: Effects of the climate variables temperature and discharge. Water Res. 47, 6585–6595. https://doi.org/10.1016/j.watres.2013.08.028

Duval, T.P., Hill, A.R., 2006. Influence of stream bank seepage during low-flow conditions on riparian zone hydrology: INFLUENCE OF BANK SEEPAGE. Water Resour. Res. 42, n/a–n/a. https://doi.org/10.1029/2006WR004861

Eimers, M.C., Buttle, J., Watmough, S.A., 2008. Influence of seasonal changes in runoff and extreme events on dissolved organic carbon trends in wetland- and upland-draining streams. Can. J. Fish. Aquat. Sci. 65, 796–808. https://doi.org/10.1139/f07-194

Fasching, C., Ulseth, A.J., Schelker, J., Steniczka, G., Battin, T.J., 2015. Hydrology controls dissolved organic matter export and composition in an Alpine stream and its hyporheic zone. Limnol. Oceanogr. https://doi.org/10.1002/lno.10232

Findlay, S., 1995. Importance of surface-subsurface exchange in stream ecosystems: the hyporheic zone. Limnol. Oceanogr. 40, 159–164.

Fukada, T., Hiscock, K.M., Dennis, P.F., Grischek, T., 2003. A dual isotope approach to identify denitrification in groundwater at a river-bank infiltration site. Water Res. 37, 3070–3078. https://doi.org/10.1016/S0043-1354(03)00176-3

Gift, D.M., Groffman, P.M., Kaushal, S.S., Mayer, P.M., 2010. Denitrification Potential, Root Biomass, and Organic Matter in Degraded and Restored Urban Riparian Zones. Restor. Ecol. 18, 113–120. https://doi.org/10.1111/j.1526-100X.2008.00438.x

Grischek, T., Hiscock, K.M., Metschies, T., Dennis, P.F., Nestler, W., 1998. Factors affecting denitrification during infiltration of river water into a sand and gravel aquifer in Saxony, Germany. Water Res. 32, 450–460. https://doi.org/10.1016/S0043-1354(97)00208-X

Grizzetti, B., Bouraoui, F., Aloe, A., European Commission, Joint Research Centre, Institute for Environment and Sustainability, 2007. Spatialised European nutrient balance. EUR-OP, Luxembourg.

Harvey, J.W., Bencala, K.E., 1993. The effect of streambed topography on surface-subsurface water exchange in mountain catchments. Water Resour. Res. 29, 89–98.

Hedin, L.O., Fischer, J.C. von, Ostrom, N.E., Kennedy, B.P., Brown, M.G., Robertson, G.P., 1998. Thermodynamic Constraints on Nitrogen Transformations and Other Biogeochemical Processes at Soil-Stream Interfaces. Ecology 79, 684–703. https://doi.org/10.2307/176963

Heeren, D.M., Fox, G.A., Fox, A.K., Storm, D.E., Miller, R.B., Mittelstet, A.R., 2014. Divergence and flow direction as indicators of subsurface heterogeneity and stage-dependent storage in alluvial floodplains. Hydrol. Process. 28, 1307–1317. https://doi.org/10.1002/hyp.9674

Hefting, M., Clément, J.C., Dowrick, D., Cosandey, A.C., Bernal, S., Cimpian, C., Tatur, A., Burt, T.P., Pinay, G., 2004. Water table elevation controls on soil nitrogen cycling in riparian wetlands along a European climatic gradient. Biogeochemistry 67, 113–134. https://doi.org/10.1023/B:BIOG.0000015320.69868.33

Hill, A.R., 1996. Nitrate Removal in Stream Riparian Zones. J. Environ. Qual. 25, 743–755. https://doi.org/10.2134/jeq1996.00472425002500040014x

Hill, A.R., Devito, K.J., Campagnolo, S., Sanmugadas, K., 2000. Subsurface Denitrification in a Forest Riparian Zone: Interactions between Hydrology and Supplies of Nitrate and Organic Carbon. Biogeochemistry 51, 193–223.

Hill, A.R., Labadia, C.F., Sanmugadas, K., 1998. Hyporheic zone hydrology and nitrogen dynamics in relation to the streambed topography of a N-rich stream. Biogeochemistry 42, 285–310. https://doi.org/10.1023/A:1005932528748

Hoffmann, C.C., Berg, P., Dahl, M., Larsen, S.E., Andersen, H.E., Andersen, B., 2006. Groundwater flow and transport of nutrients through a riparian meadow – Field data and modelling. J. Hydrol. 331, 315–335. https://doi.org/10.1016/j.jhydrol.2006.05.019

Hosono, T., Alvarez, K., Lin, I.-T., Shimada, J., 2015. Nitrogen, carbon, and sulfur isotopic change during heterotrophic (Pseudomonas aureofaciens) and autotrophic (Thiobacillus denitrificans) denitrification reactions. J. Contam. Hydrol. 183, 72–81. https://doi.org/10.1016/j.jconhyd.2015.10.009

Hosono, T., Tokunaga, T., Kagabu, M., Nakata, H., Orishikida, T., Lin, I.-T., Shimada, J., 2013. The use of δ15N and δ18O tracers with an understanding of groundwater flow dynamics for evaluating the origins and attenuation mechanisms of nitrate pollution. Water Res. 47, 2661–2675. https://doi.org/10.1016/j.watres.2013.02.020

Jacobs, L.A., von Gunten, H.R., Keil, R., Kuslys, M., 1988. Geochemical changes along a river-groundwater infiltration flow path: Glattfelden, Switzerland. Geochim. Cosmochim. Acta 52, 2693–2706. https://doi.org/10.1016/0016-7037(88)90038-5

Jawitz, J.W., Mitchell, J., 2011. Temporal inequality in catchment discharge and solute export. Water Resour. Res. 47, W00J14. https://doi.org/10.1029/2010WR010197

Kaplan, L.A., Newbold, J.D., 2000. 10 - Surface and Subsurface Dissolved Organic Carbon, in: Mulholland, J.B.J.J. (Ed.), Streams and Ground Waters, Aquatic Ecology. Academic Press, San Diego, pp. 237–258.

Kellogg, D.Q., Gold, A.J., Groffman, P.M., Addy, K., Stolt, M.H., Blazejewski, G., 2005. In situ ground water denitrification in stratified, permeable soils underlying riparian wetlands. J. Environ. Qual. 34, 524–533.

Kendall, C., McDonnell, J.J. (Eds.), 1998. Isotope tracers in catchment hydrology. Elsevier, Amsterdam ; New York.

Kirsch, R., 2008. Groundwater Geophysics: A Tool for Hydrogeology, 2nd ed. 2009. ed. Springer, Berlin.

Knöller, K., Trettin, R., Strauch, G., 2005. Sulphur cycling in the drinking water catchment area of Torgau–Mockritz (Germany): insights from hydrochemical and stable isotope investigations. Hydrol. Process. 19, 3445–3465. https://doi.org/10.1002/hyp.5980

Knöller, K., Vogt, C., Haupt, M., Feisthauer, S., Richnow, H.-H., 2011. Experimental investigation of nitrogen and oxygen isotope fractionation in nitrate and nitrite during denitrification. Biogeochemistry 103, 371–384. https://doi.org/10.1007/s10533-010-9483-9

Kothawala, D.N., Ji, X., Laudon, H., Ågren, A.M., Futter, M.N., Köhler, S.J., Tranvik, L.J., 2015. The relative influence of land cover, hydrology, and in-stream processing on the composition of dissolved organic matter in boreal streams: Stream DOM Composition. J. Geophys. Res. Biogeosciences 120, 1491–1505. https://doi.org/10.1002/2015JG002946

Lambert, T., Pierson-Wickmann, A.-C., Gruau, G., Thibault, J.-N., Jaffrezic, A., 2011. Carbon isotopes as tracers of dissolved organic carbon sources and water pathways in headwater catchments. J. Hydrol. 402, 228–238. https://doi.org/10.1016/j.jhydrol.2011.03.014

Leenheer, J.A., Croué, J.-P., 2003. Peer Reviewed: Characterizing Aquatic Dissolved Organic Matter. Environ. Sci. Technol. 37, 18A–26A. https://doi.org/10.1021/es032333c

Mariotti, A., Landreau, A., Simon, B., 1988. 15N isotope biogeochemistry and natural denitrification process in groundwater: Application to the chalk aquifer of northern France. Geochim. Cosmochim. Acta 52, 1869–1878. https://doi.org/10.1016/0016-7037(88)90010-5

Mayer, P.M., Reynolds, S.K., McCutchen, M.D., Canfield, T.J., 2007. Meta-Analysis of Nitrogen Removal in Riparian Buffers. J. Environ. Qual. 36, 1172. https://doi.org/10.2134/jeq2006.0462

Mengis, M., Schif, S.L., Harris, M., English, M.C., Aravena, R., Elgood, R., MacLean, A., 1999. Multiple Geochemical and Isotopic Approaches for Assessing Ground Water NO3− Elimination in a Riparian Zone. Ground Water 37, 448–457. https://doi.org/10.1111/j.1745-6584.1999.tb01124.x

Meybeck, M., 1982. Carbon, Nitrogen, and Phosphorus Transport by World Rivers. Am J Sci U. S. 282:4. https://doi.org/10.2475/ajs.282.4.401

Mueller, C., Krieg, R., Merz, R., Knöller, K., 2015. Regional nitrogen dynamics in the TERENO Bode River catchment, Germany, as constrained by stable isotope patterns. Isotopes Environ. Health Stud. 1–14. https://doi.org/10.1080/10256016.2015.1019489

Mueller, C., Zink, M., Samaniego, L., Krieg, R., Merz, R., Rode, M., Knöller, K., 2016. Discharge Driven Nitrogen Dynamics in a Mesoscale River Basin As Constrained by Stable Isotope Patterns. Environ. Sci. Technol. 50, 9187–9196. https://doi.org/10.1021/acs.est.6b01057

Musolff, A., Schmidt, C., Selle, B., Fleckenstein, J.H., 2015. Catchment controls on solute export. Adv. Water Resour. 86, 133–146. https://doi.org/10.1016/j.advwatres.2015.09.026

Naeher, S., Huguet, A., Roose-Amsaleg, C.L., Laverman, A.M., Fosse, C., Lehmann, M.F., Derenne, S., Zopfi, J., 2015. Molecular and geochemical constraints on anaerobic ammonium oxidation (anammox) in a riparian zone of the Seine Estuary (France). Biogeochemistry 123, 237–250. https://doi.org/10.1007/s10533-014-0066-z

Ostrom, N.E., Hedin, L.O., Von Fischer, J.C., Robertson, G.P., 2002. Nitrogen transformations and NO3- removal at a soil–stream interface: a stable isotope approach. Ecol. Appl. 12, 1027–1043.

Peter, S., Rechsteiner, R., Lehmann, M.F., Brankatschk, R., Vogt, T., Diem, S., Wehrli, B., Tockner, K., Durisch-Kaiser, E., 2012. Nitrate removal in a restored riparian groundwater system: functioning and importance of individual riparian zones. Biogeosciences 9, 4295–4307. https://doi.org/10.5194/bg-9-4295-2012

Pfenning, K.S., McMahon, P.B., 1997. Effect of nitrate, organic carbon, and temperature on potential denitrification rates in nitrate-rich riverbed sediments. J. Hydrol. 187, 283–295.

Pinay, G., Ruffinoni, C., Wondzell, S., Gazelle, F., 1998. Change in Groundwater Nitrate Concentration in a Large River Floodplain: Denitrification, Uptake, or Mixing? J. North Am. Benthol. Soc. 17, 179–189. https://doi.org/10.2307/1467961

Puckett, L.J., 2004. Hydrogeologic controls on the transport and fate of nitrate in ground water beneath riparian buffer zones: results from thirteen studies across the United States. Water Sci. Technol. 49, 47–53.

Puckett, L.J., Hughes, W.B., 2005. Transport and Fate of Nitrate and Pesticides. J. Environ. Qual. 34, 2278. https://doi.org/10.2134/jeq2005.0109

Raeke, J., Lechtenfeld, O.J., Tittel, J., Oosterwoud, M.R., Bornmann, K., Reemtsma, T., 2017. Linking the mobilization of dissolved organic matter in catchments and its removal in drinking water treatment to its molecular characteristics. Water Res. 113, 149–159. https://doi.org/10.1016/j.watres.2017.01.066

Ranalli, A.J., Macalady, D.L., 2010. The importance of the riparian zone and in-stream processes in nitrate attenuation in undisturbed and agricultural watersheds – A review of the scientific literature. J. Hydrol. 389, 406–415. https://doi.org/10.1016/j.jhydrol.2010.05.045

Rivett, M.O., Buss, S.R., Morgan, P., Smith, J.W.N., Bemment, C.D., 2008. Nitrate attenuation in groundwater: A review of biogeochemical controlling processes. Water Res. 42, 4215–4232. https://doi.org/10.1016/j.watres.2008.07.020

Sawyer, A.H., M. B. Cardenas, Bomar, A., Mackey, M., 2009. Impact of dam operations on hyporheic exchange in the riparian zone of a regulated river. Hydrol. Process. 23, 2129–2137. https://doi.org/10.1002/hyp.7324

Schwientek, M., Einsiedl, F., Stichler, W., Stögbauer, A., Strauss, H., Maloszewski, P., 2008. Evidence for denitrification regulated by pyrite oxidation in a heterogeneous porous groundwater system. Chem. Geol. 255, 60–67. https://doi.org/10.1016/j.chemgeo.2008.06.005

Sigman, D.M., Casciotti, K.L., Andreani, M., Barford, C., Galanter, M., Böhlke, J.K., 2001. A Bacterial Method for the Nitrogen Isotopic Analysis of Nitrate in Seawater and Freshwater. Anal. Chem. 73, 4145–4153. https://doi.org/10.1021/ac010088e

Simmons, R.C., Gold, A.J., Groffman, P.M., 1992. Nitrate Dynamics in Riparian Forests: Groundwater Studies. J. Environ. Qual. 21, 659–665. https://doi.org/10.2134/jeq1992.00472425002100040021x

Stumm, W., Morgan, J.J., 2012. Aquatic Chemistry: Chemical Equilibria and Rates in Natural Waters. John Wiley & Sons.

Trauth, N., Fleckenstein, J.H., 2017. Single discharge events increase reactive efficiency of the hyporheic zone. Water Resour. Res. https://doi.org/10.1002/2016WR019488

Valett, H.M., Morrice, J.A., Dahm, C.N., Campana, M.E., 1996. Parent lithology, surface–groundwater exchange, and nitrate retention in headwater streams. Limnol. Oceanogr. 41, 333–345. https://doi.org/10.4319/lo.1996.41.2.0333

Vervier, P., Dobson, M., Pinay, G., 1993. Role of interaction zones between surface and ground waters in DOC transport and processing: considerations for river restoration. Freshw. Biol. 29, 275–284. https://doi.org/10.1111/j.1365-2427.1993.tb00763.x

Vidon, Hill, A.R., 2004a. Denitrification and patterns of electron donors and acceptors in eight riparian zones with contrasting hydrogeology. Biogeochemistry 71, 259–283. https://doi.org/10.1007/s10533-004-9684-1

Vidon, Hill, A.R., 2004b. Landscape controls on nitrate removal in stream riparian zones. Water Resour. Res. 40. https://doi.org/10.1029/2003WR002473

Vidon, P., Marchese, S., Rook, S., 2017. Impact of Hurricane Irene and Tropical Storm Lee on riparian zone hydrology and biogeochemistry. Hydrol. Process. 31, 476–488. https://doi.org/10.1002/hyp.11045

Vieweg, M., Kurz, M.J., Trauth, N., Fleckenstein, J.H., Musolff, A., Schmidt, C., 2016. Estimating time-variable aerobic respiration in the streambed by combining electrical conductivity and dissolved oxygen time series: Variable Respiration in the Streambed. J. Geophys. Res. Biogeosciences 121, 2199–2215. https://doi.org/10.1002/2016JG003345

Wang, S., Zhu, G., Peng, Y., Jetten, M.S.M., Yin, C., 2012. Anammox Bacterial Abundance, Activity, and Contribution in Riparian Sediments of the Pearl River Estuary. Environ. Sci. Technol. 46, 8834–8842. https://doi.org/10.1021/es3017446

Wold, S., Sjöström, M., Eriksson, L., 2001. PLS-regression: a basic tool of chemometrics. Chemom. Intell. Lab. Syst., PLS Methods 58, 109–130. https://doi.org/10.1016/S0169-7439(01)00155-1

Wollschläger, U., Attinger, S., Borchardt, D., Brauns, M., Cuntz, M., Dietrich, P., Fleckenstein, J.H., Friese, K., Friesen, J., Harpke, A., Hildebrandt, A., Jäckel, G., Kamjunke, N., Knöller, K., Kögler, S., Kolditz, O., Krieg, R., Kumar, R., Lausch, A., Liess, M., Marx, A., Merz, R., Mueller, C., Musolff, A., Norf, H., Oswald, S.E., Rebmann, C., Reinstorf, F., Rode, M., Rink, K., Rinke, K., Samaniego, L., Vieweg, M., Vogel, H.-J., Weitere, M., Werban, U., Zink, M., Zacharias, S., 2017. The Bode hydrological observatory: a platform for integrated, interdisciplinary hydro-ecological research within the TERENO Harz/Central German Lowland Observatory. Environ. Earth Sci. 76, 29. https://doi.org/10.1007/s12665-016-6327-5

Wondzell, S.M., Swanson, F.J., 1999. Floods, channel change, and the hyporheic zone. Water Resour. Res. 35, 555–567. https://doi.org/10.1029/1998WR900047

Zarnetske, J.P., Haggerty, R., Wondzell, S.M., Baker, M.A., 2011. Labile dissolved organic carbon supply limits hyporheic denitrification. J. Geophys. Res. 116. https://doi.org/10.1029/2011JG001730

HIGHLIGHTS

to manuscript “River water infiltration enhances denitrification efficiency in riparian groundwater”

by Trauth et. al.

1. Hydrochemical and isotopic data of 2-year sampling period in a riparian zone
2. Temperature can explain 67.8% of the variance in DO and 66.2% in $\delta^{15}N$
3. The higher the river water content in groundwater the higher is $\delta^{15}N$ enrichment
4. Reactions depend on bioavailable carbon delivered by infiltrating river water